universität wien

DIPLOMARBEIT

Titel der Diplomarbeit

Cross Sectional Nanoindentation as Means of Adhesion Characterisation at the Wood-Adhesive Bond Line

angestrebter akademischer Grad

Magister der Naturwissenschaften (Mag. rer.nat.)

Verfasser:	Michael Obersriebnig
Matrikel-Nummer:	0500734
Studienrichtung:	Physik
Betreuer:	Ao.Univ.Prof. Dipl.-Ing. Dr.nat.techn. Wolfgang Gindl-Altmutter

Wien, 04/2011

Danksagung

Diese Diplomarbeit entstand im Zeitraum Juni 2010 - April 2011 am Institut für Holzforschung der Universtität für Bodenkultur in Wien.

Ich möchte mich an dieser Stelle bei allen bedanken, die mich beim Verfassen dieser Arbeit unterstützt haben, insbesondere bei meinem Betreuer Prof. Wolfgang Gindl-Altmutter. Besonderer Dank gilt auch Dr. Johannes Konnerth für seine fachliche Betreuung, Beratung und technische Unterstützung sowie DI Stefan Veigel für seine Mithilfe und Unterstützung. Weiters geht mein Dank an Prof. Alfred Teischinger für die Möglichkeit, am Institut für Holzforschung meine Arbeit zu verfassen.

Allgemein gilt ein großer Dank den Mitarbeitern am Institut für Holzforschung und WoodK Plus für das nette und kollegiale Umfeld, in dem ich arbeiten konnte.

An der TU Wien geht mein Dank vor allem auch an Dr. Olaf Lahayne und Frau Ewa Spiesz für die Betreuung bei technischen Problemen.

Ein großer Dank gilt besonders meinen Freunden und Kollegen am Institut für Physik, die mir wo nötig zur Seite standen und die über die Jahre einen großen Anteil daran haben, dass diese Arbeit überhaupt begonnen werden konnte. Insbesondere erwähnen will ich hier auch Bernadette Rosati, Matthias Bönisch und Gerhard König für das Korrekturlesen von Teilen der Arbeit und das Geben von wertvollen Hinweisen.

Abschließend möchte ich mich bei meiner Familie und meinen Eltern bedanken, deren Beitrag man wohl nicht hoch genug einschätzen kann und die mir das Studium und damit diese Arbeit überhaupt erst ermöglichten.

Abstract

The aim of this work was to find a way to apply the method of cross sectional nanoindentation, introduced by Sánchez *et al.*, to wood-adhesive interfaces. In a first step, samples were subjected to various surface treatments with silanes to artificially lower the adhesion strength with the adhesive used. Performing contact angle measurements for a first characterisation of treatment effectiveness, significant changes were found for all modifications. In the following shear test, one set of samples displayed a shear strength close to zero. Thus, a good basis for measuring the specific adhesion was given. Nanoindentation experiments were performed directly at the wood-adhesive bond line, where the adhesive was in intimate contact with the inner cell wall of wood cells. Results from a first experiment displayed a clear trend of decreasing adhesion for increasing contact angles, in accordance with the shear test. In a second experiment, indents were performed using varying load functions, to analyse their influence on the experiment. Results showed a strong hysteretic behaviour of the force-displacement curve for displacement controlled multi-load functions due to additional visco-elastic deformation, causing an increase in the measured specific work of indentation as well as the specific work of adhesion, which varied between 80-170J/m². However, all results showed the expected significant decrease in adhesive strength. Material characterisation of the cell wall and the adhesive showed no similar trends for their respective mechanical properties, thus allowing to discard the possibility of artefacts. With these findings, it was concluded that cross sectional nanoindentation can indeed be applied to wood-adhesive interfaces and should provide new insights into the nature of adhesive bonds in wood-based composites.

Zusammenfassung

Das Ziel dieser Arbeit war es, ”cross sectional nanoindentation”, eine Methode der Adhäsionsmessung erstmals vorgestellt von Sánchez *et al.*, an einer Holz-Klebstoff Grenfläche anzuwenden. In einem ersten Schritt wurden die Proben dre verschiedenen Oberflächenbehandlungen mit Silanen unterzogen, um derart die Adhäsion zum verwendeten Leim herabzusetzen. Eine Kontaktwinkelmessung an allen Proben bestätigte die Effektivität der Behandlung und zeigte signifikante Änderungen des Kontaktwinkels im Vergleich zu einer unbehandelten Referenz. Diese Änderung des Kontaktwinkels wurde durch einen Zugschertest bestätigt. Für alle Probentypen nahm die maximale Zugspannung signifikant ab und lag für einen Probentyp sogar bei fast Null. Somit waren die Vorraussetzungen zur Messung der spezifischen Adhäsion gegeben. Die Nanoindenter-Messungen wurden an der Holz-Leim-Grenzlinie durchgeführt, an Stellen wo ein vollständiger Kontakt des Leims mit der Zellinnenwand des Holzes gegeben war. Die Ergebnisse eines ersten Versuchs zeigten in Analogie zum Zugschertest eine Abnahme der Adhäsion bei Proben mit höherem Kontaktwinkel. In einem zweiten Versuch wurden verschiedene Beladefunktionen für die Indents verwendet, um deren Einfluss auf das Experiment zu untersuchen. Hierbei zeigte sich ein starker Hysterese-Effekt bei mehrstufigen weggesteuerten Beladefunktionen aufgrund zusätzlicher visco-elastischer Verformung. Das führte zu einer Zunahme der gemessenen spezifischen Indentationsarbeit als auch der spezifischen Adhäsionsarbeit, wobei letztere Werte von 80-170J/m² annahm. Alle Ergebnisse wiesen jedoch die erwartete signifikante Abnahme der Adhäsion auf. Eine Charakterisierung der Materialeigenschaften von Zellwand und Leim zeigte keine ähnlichen Trends, womit die Möglichkeit von Artefakten verworfen werden konnte. Die gefundenen Ergebnisse erlauben den Schluss, dass die Methode der ”cross sectional nanoindentation” an Holz-Leim-Grenzflächen eingesetzt werden

kann. Sie sollte somit neue Einsichten in die Natur von adhäsiven Verbindungen in holz-basierten Verbunden ermöglichen.

Contents

Motivation

Be it composite materials, using an adhesive tape, painting a wall or various medical applications, to name just a few examples - adhesion and adhesion phenomena surround us and are very important in technics and everyday life. However, even though adhesion plays a crucial role in many fields of science and technology, the knowledge about the principles of adhesion leaves a lot to be desired.

Still a rather young scientific discipline, in recent years a great amount of energy has been put into development and interpretation of adhesion measurement techniques on a microscopic lengthscale. Considering adhesion to natural materials, a few methods for measuring adhesion to fibres and modelling properties of fiber-based composites exist. However, for wood and wood particles, up to date no methods of micro-adhesion measurement existed.

Therefore, the aim of this thesis was the application of an adhesion measuring technique developed for micro-adhesion measurement in integrated circuits to wood-adhesive interfaces.

Theoretical Section

Adhesion

Being at the intersection of many different fields of studies, different theories were stated trying to explain adhesive bonding. Treating different aspects of adhesion, it is usually not one single theory which explains a specific case of adhesive bonding but, being complementary to some point in assuming different interactions at the interface, a number of them. Those theories allow to make some predictions on adhesive quality and explain outcomes of adhesion tests. However, those approaches are mostly empirical. Up to date, we still lack a general theory of adhesion which properly explains adhesion phenomena on a molecular level. Therefore, to improve our knowledge, it is crucial to gain new information through experimental data.

This brings attention to another important factor, adhesion measuring methods. Standard adhesion tests mostly work on a macroscopic scale. They are easier to set up and until some 20-30 years ago, there were simply no alternative methods available. While it can be seen as an advantage that, due to the macroscopic scale, those tests give the mean strength over a rather large sample area, this can also be considered a problem, as it limits the gained information. There are various properties of adherents, e.g. surface roughness or local destribution of the adhesive, which can take an effect on the measured adhesive strength, as will be explained below. With macroscopic methods it is not possible to properly separate the measured work into 'specific' adhesion due to molecular interactions at the interface and influences from different structural properties. Therefore, it became and still is a necessity to improve testing methods in order to provide measurements on a smaller scale.

In the following, short summaries of the existing theories of adhesion are given as well as a of selection of adhesion tests on the macroscopic and microscopic level.

Theories of Adhesion

Thermodynamic/Adsorption Theory

The adsorption or thermodynamic theory is the most widely used adhesion theory and will therefore be treated in some detail.

It states interatomic forces as the foundation for adhesion (however, it does not make any further assumptions concerning the specific nature of these forces). Therefore, to achieve good adhesion, intimate contact between adherent and adhesive must be reached. This can be seen as a basic criterion also for the other theories discribed below, which is why the adsorption theory takes a special place among adhesion theories.

The formation of an adhesive bond generally goes through a solid-liquid phase first, where an adhesive in a liquid state is brought onto the adherent. With this, adhesion criteria basically become criteria of good wettability. Linking the wettability to the work of adhesion W, which in turn allows for an estimate of the adhesion strength G, one can predict the quality of an adhesive bond.

Young (1805) links the contact angle Θ, as criterion for wettability, to the surface energy γ of the phases in contact (1) ,

$$\gamma_{SV} - \gamma_{SL} = \gamma_{LV} \cos\Theta \tag{1}$$

where the indices S, L and V stand for the solid, liquid and vaporous phase (figure 1). For spontaneous or total wetting Θ equals zero. Therefore, a condition for total wetting to occur is

$$\gamma_{SV} \geqq \gamma_{SL} + \gamma_{LV}$$

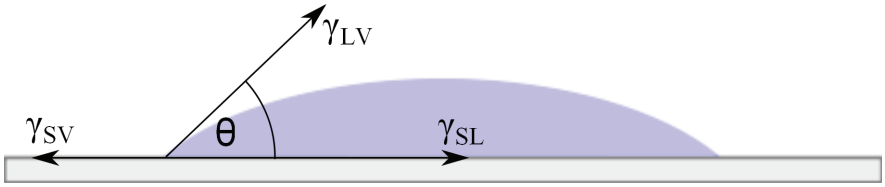

Figure 1: Illustration of Young's equation

This has lead to the definition of the spreading coefficient S as indicator of the wetting properties of a system (2).

$$S = \gamma_{SV} - \gamma_{SL} - \gamma_{LV} \tag{2}$$

For values of S equal to or larger than zero, total wetting occurs while it is only partial for negative values.

Dupré (1869) has stated a relation between the adhesion energy W and the surface energies of the adherents. Two solids 1 and 2 in contact over an area A have the energy

$$U = U_0 + \gamma_{12} A$$

where γ_{12} is the interfacial energy. With the solids seperated, the energy of the system becomes

$$U = U_0 + (\gamma_1 + \gamma_2) A$$

with γ_1 and γ_2 the respective surface energies (to be accurate, those in vacuum). Therefore, the specific energy per area to seperate the two objects (isothermally and reversibly) is

$$W = \gamma_1 + \gamma_2 - \gamma_{12} \tag{3}$$

This is called the *Dupré's energy of adhesion.* Combining this with (1) and rewriting the indices 1 and 2 to those at the respective phase-boundaries, one gets the specific adhesion energy of a solid-liquid system as

$$W_{SL} = \gamma_{SV} + \gamma_{LV} - \gamma_{SL} = \gamma_{LV}\left(1 + \cos\Theta\right) \tag{4}$$

Work by Schultz *et al.* (1977) suggests that γ may be expressed as sum of a dispersive and a polar component which in turn may be expressed as twice the geometric mean of the respective components. This allows for the specific work of adhesion to be expressed as

$$W_{12} = 2\left(\gamma_1^D \gamma_2^D\right)^{1/2} + 2\left(\gamma_1^P \gamma_2^P\right)^{1/2} \tag{5}$$

where the superscripts indicate the dispersive and polar components, respectively.

Fowkes and co-workers (Fowkes and Maruchi, 1977; Fowkes and Mostafa, 1978; Fowkes, 1984, 1987) have accounted in their work for Lewis acid-base interactions while neglecting the polar component, which usually contributes only a minor part of the total bond strength. By relating the energy of acid-base interactions to the change in enthalpy ΔH^{ab}, they get the work of adhesion as

$$W_{12} = 2\left(\gamma_1^D \gamma_2^D\right)^{1/2} + f\left(-\Delta H^{ab}\right) n^{ab} \tag{6}$$

where f is a factor that converts enthalpy into free energy and n^{ab} is the density of acid-base bonds per unit area.

The *model of multiplying factors* relates the adhesion strength to the work of adhesion. Proposed primarily by Gent and Schultz (1971), it states the adhesion strength simply as a product of the work of adhesion or 'specific adhesion' and a loss function Φ, which takes into account the energy dissipated irreversibly in viscoelastic or plastic deformations (7),

$$G = W\Phi\left(v, T\right) \tag{7}$$

where v is the crack propagation rate and T is the temperature. The specific form of equation (7) varies with the problem at hand where different expressions for Φ and W might be useful. Since usually the main contributor to

adhesion strength comes from viscoelastic and plastic losses, especially Φ has to be modified according to one's prerequisites while W is often substituted by the more convenient intrinsic fracture energy G_0, a treshold value which is reached for $\Phi \rightarrow 1$ and is about 100-1000 times larger than the pure thermodynamic work of adhesion W due to effects on a molecular length scale.

Mechanical Interlocking

This theory, proposed by McBain and Hopkins (1925), assumes interlocking of the surface structures as a contributor to adhesion strength. Therefore, rough structures should have better adhesive qualities than smooth surfaces. While this is generally true, there are known cases that show a decrease of adhesion for roughening up the surface. This led to the theory falling out of favor around the 1950s. Nowadays it is reasoned that rather than mechanical interlocking an increase in contact area and therefore more interaction causes the improved adhesion for rough surfaces, and while mechanical interlocking can indeed occur, its effect is usually only minor.

Packham (2003) writes on the topic or surface roughness and thereby increased contact area, that the main difficulty lies in finding a proper way of defining it. For roughness on a micrometer scale, a simple solution would be to measure the actual surface area with a probe and define an area ratio as true surface area to projected surface area. With this, the measured adhesion strength could be normalised and variations in surface roughness could be accounted for. However, this approach becomes more and more difficult moving to roughness on nanometer or even atomic scale. In the limit of a fractal roughness, the measured surface area depends on the fineness of the probe and no valid true surface area could be given. Also, for roughness at a very small scale, the solvent accessible area strongly depends on viscosity of the adhesive and wettability of the adherent. Therefore, the best measure for surface area remains the projected area with an implicit effect of an increased contact for rough structures.

Electronic Theory

This theory, introduced by Deryagin and Krotova (1948), suggests an electron transfer between substrate and adhesive as cause of adhesion. However, contradictions have been found which strongly question this assumption (Wake, 1982). Basically, it stands to reason that electronic phenomena found during debonding processes are rather the consequence than the cause of strong adhesion. A further point of criticism of this theory is that it does not include viscoelastic and plastic dissipation of energy.

Chemical Bonding Theory

Chemical bonds can greatly contribute to adhesion, having a considerably higher bond strength than the purely physical van der Waals and hydrogen bonds (100 to 1000 kJ/mol compared to less than 50 kJ/mol). They are especially important where adhesion promoters or coupling agents are used, chemicals which act as a bridge between a substrate and an adhesive which normally would not bond well. Several experiments support the assumption of chemicals bonding, stating a clear relationship between the adhesion strength G and the number of bonds v per unit area. However, different sources are contradictory as to the nature of this relationship, stating the dependence of G on v as linear (A. N. Gent and J. Schultz, 1971; Delescluse *et al.*, 1984) or quadratic (Brown, 1989; Brown *et al.*, 1989; Brown, 1991), respectively. Also, as above mentioned, a necessary criterion for chemical bonding is an intimate contact as described by the adsorption theory. Additionally, a rough surface could increase the true contact area and by that the number of bonds per projected surface area.

Theory of Boundary Layers and Interphases

Modifications of the adhesive and the adherent near the interface lead to the formation of an interfacial zone (Schultz *et al.*, 1984; Schultz and Carré, 1984; Schultz *et al.*, 1989; Nardin *et al.*, 1991, 1993). Bikerman (1968) first treated this problem and proposed cohesive failure in this modified zone, the so-called interphase, as the main failure mechanism and therefore the

strength of this interphase as main criterion for adhesive strength. This theory has been critisised since purely adhesive failure does occur and even where cohesive failure is observed, this does not necessarily indicate failure of the interphase. Still, the formation of interphases (the diameter of which ranges between a few angstroms and several micrometers) has caught attention and has to be considered when analysing an adhesive bond as it can greatly influence the properties of the bond.

Diffusion Theory

The diffusion theory assumes mutual diffusion of macromolecules (thus creating an interphase) across an adhesively bonded interface as reason for adhesion. This means that the bond strength should depend on time and temperature as well as other factors like the molecular weight and nature of the adherents. Vasenin and Saltykova (1975) have developed a model, based on Fick's law, descriping the dependence of the adhesion strength G (measured with a peel test) on above factors, especially a dependence on the contact time $t^{\frac{1}{4}}$, which was also found in experiments. These results, however, were contradicted by several studies (Jud *et al.*, 1981; Prager and Tirrell, 1981; Kim and Wool, 1983) which found a clear dependence of G on $t^{\frac{1}{2}}$. No general agreement was found for trends concerning the molecular mass.

Nontheless, diffusion can be assumed to greatly contribute to adhesion at polymer-polymer interfaces and is especially important for self healing processes in polymer-polymer bonds (Jud *et al.*, 1981; Kim and Wool, 1983).

Adhesion Tests

Adhesion test methods in general are destructive in nature, meaning an adhesive or an adhesively bonded structure is tested by applying a force until collapse of the adhesive bond. The strength or quality of the bond is then defined through the applied peak force or the total energy necessary for collapsing the bond. This raises the problem of not actually measuring adhesion, but a parameter which is closely related, but influenced by a number of factors. Those of course include the chemical properties of the adhesive

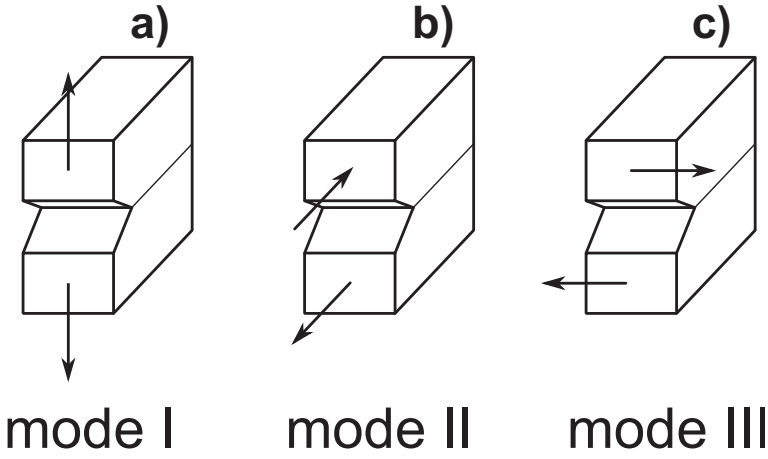

Figure 2: Schematic represantation of force direction for different fracture modes; a) mode I: force normal to bonded area, ”opening”; b) mode II: shear tension in plane direction; c) mode III: excentric torsion load in plane direction, ”tearing”

and adherent, but also structural parameters like surface roughness and structure, local distribution of the adhesive or, for composite materials, the size of the reinforcement material. As has been explained above, the most part of the energy spent on breaking an adhesive bond is actually due to plastic and viscoelastic losses of the bonded materials. With different contact zones, the deformed volume and, along with it, the measured work of debonding greatly changes.

Another important factor is the load direction. There are three main modes of failure, depending on the load direction, those being normal load (a), leading to ”opening”, in-plane shear load (b), leading to ”sliding off” of the structure and an excentric torsion load (c), leading to ”tearing” (figure 2). Usually, failure is associated with a mixture of these three ”pure” modes. It is easily understandable, that different load directions lead to different types of failure, which can greatly vary in strength. Therefore, for an adhesion test, it is necessary to mirror the expected operating load. For scientific purposes, pure single-mode failure is preferably to better relate results to different parameters. Models then have to consider and be able to explain different behaviour under different load modes.

As the requirements for adhesives and the typical load type of an adhesive bond greatly vary with the field of application, a great number of methods

to test and characterise adhesives has been developed. With advances in technology, available methods have moved from a macroscopic scale to a microscopic scale, sometimes by refining an existing method, sometimes by searching new approaches. The advantages of macroscopic methods are typically an easier sample preparation, faster and possibly automated testing and usually straight forward data analysis. Due to the large scale the results are averaged over a comparably large area, an advantage for technical applications where usually the strength of a given structure is of interest. For scientific applications however, trying to explain the reasons for a specific behaviour, pure macroscopic testing states a problem due to being influenced by to many parameters, not all of them controllable.

In this section, a short summary of a number of methods for adhesion characterisation is given, together with their usual field of application, to give an idea of the broadness of this field and the problems when trying to measure and define adhesion.

Macroscopic Adhesion Tests

- SHEAR TEST - Maybe the most widely used method, the shear test is a standard method for comparing adhesive bonds. Samples are prepared with a well defined overlap, then, by applying a tensile force at both ends, sheared off. The exact procedure for sample preparation and execution of the test is described by a large number of international standards, accounting for different test materials and fields of application or different effects on the shear strength of a bond (D1002-10; D3163-01; D5868; DIN53254; EN205; EN302-1; EN302-4). The main advantages of this method are a simple sample preparation and fast testing, as well as a good sensitivity to variations in adhesion quality. The downside when testing adhesives (as contrary to the strength of the whole structure) is a tendency to cohesive failure.
- PEEL TEST and CLIMBING DRUM PEEL TEST - The peel test takes the force necessary to peel a thin layer off a surface as measure for adhesion quality. The results are greatly influenced by the force applied and the peel rate as well as the load angle. It is the standard test method for tapes and self adherent films and sheets, with various standards treating different substrates, peel velocities and force directions.

(C794-10; D3330-04) As a disadvantage, the strong dependence on the diameter and rigidity of the peeled layer should be mentioned. The climbing drum peel test is a modification fore more rigid surfaces. The softer layer gets peeled off by winding around a rigid cylinder which enables very high peel forces.

- WEDGE TEST - (SARGENT, 2005; D3762-03, 2010) This test is especially effective in characterising the durability of adhesive bonds. It is one of the main testing techniques in aircraft construction. Two strips of the tested material are bonded together and, after curing of the adhesive, a wedge is inserted at one end of the strips, forcing the pieces apart. After measuring the crack length, the sample is exposed to a warm, wet environment for some time. The growing crack is measured periodically and characterizes the durability of the adhesive. The advantage of this method, additionally to being able to monitor changes due to temperature and humidity, is that it allows for very controlled crack propagation and usually shows mainly adhesive failure. However, this happens on cost of test duration.

Microscopic Adhesion Tests

- SCRATCH TEST - This test is used for adhesion characterisation of thin hard coatings. (EN1071-05; C1624-05) While it is originally a macroscopic test method, devised for coatings of millimetre thickness, modern testing equipment allows for layers of below a hundred nanometres thickness to be analysed. Adhesion is measured by moving a diamond tip at constant velocity across the surface coating while increasing the applied force continually. The force at which delamination or chipping of the coating occurs is a measure for the adhesive strength. The problem herein is that the delamination area cannot be measured properly. Therefore the obtained results are difficult to generalize.

- FIBER-MATRIX-ADHESION TESTS - Fiber-matrix-adhesion is an important field of studies, as it greatly influences the properties of any fibrous composite, together with the respective mechanical properties of the used materials. Therefore, a number of tests exist to measure the strength of the bond (Zhandarov and Mäder, 2005). The single-fibre pull-out test derives the adhesion strength as the force (or energy)

necessary for debonding of a well-defined length of fibre embedded in a matrix (DiFrancia *et al.*, 1996). Another test method is the microbond technique, wherein a single dropplet of an adhesive gets sheared off the fibre at a sharp edge (Miller *et al.*, 1987). These tests are among the standard methods for measuring fibre-matrix adhesion and a lot of publications can also be found treating stress distributions and various influences on those tests.

As these summaries show, a large number of tests exist to measure and describe adhesion for different materials under various conditions. As the last paragraph shows, there are a number of methods to measure adhesion at a fibre-adhesive interface. Due to the quite simple properties of fibers in general and usually a rather narrow size distribution, those results can be generalized without great difficulties to describe the properties of fibrous composites. However, there exist no such methods as yet to characterize the interfacial adhesion for wood-based composites. Wood particles have a far more complex structure than standard technical fibres and usually a very broad size distribution of particles in wood-based composites (figure 3). Therefore, a method of measuring the adhesion at cell wall level should proove greatly beneficial, as it allows to exclude factors such as particle size or surface roughness.

Nanoindentation

Fundamentally based on Hertz's work on the elastic behaviour of solid objects (Hertz, 1895) and further developments thereof, nanoindentation (NI) in general describes a method for the characteristion of mechanical properties of an object on a submicron scale. The basic principle is the impression of a very rigid indenter tip (usually diamond) into the test object. While the same is true for macroscopic measurements of hardness, simultanous collection of displacement and load data allows for the high spatial resolution. Analysis of the load displacement curve allows for calculation of hardness and modulus of elasticity of the examined object.

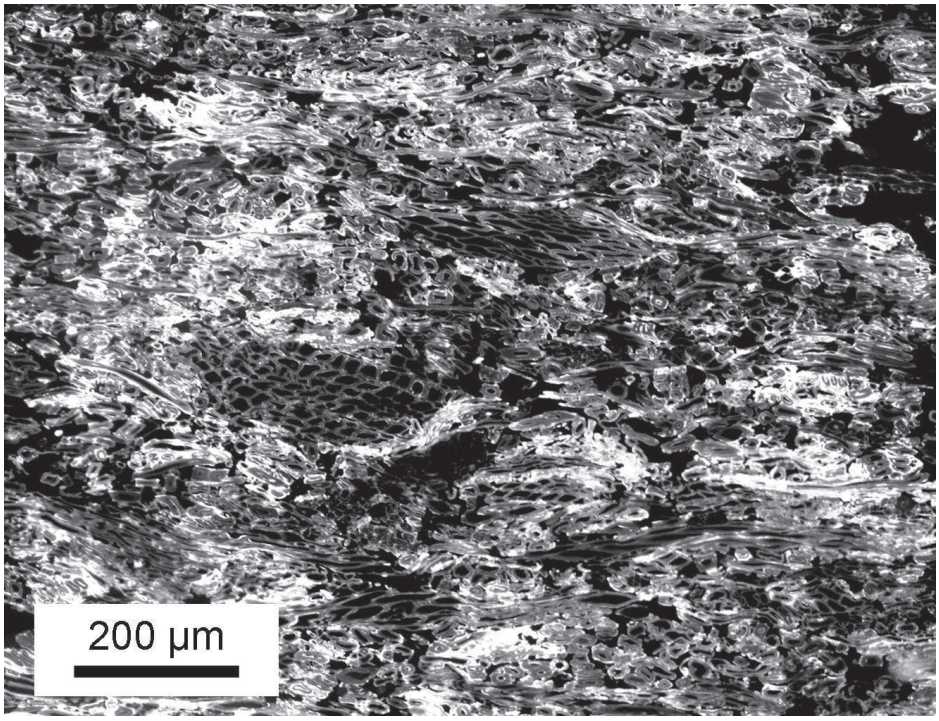

Figure 3: Microstructure of a medium density fibreboard, a representative wood-based composite. Regions containing urea-formaldehyde adhesive polymer are highlighted by staining with a fluorescent dye. (W. Gindl-Altmutter, private communication)

While this method seems quite straight forward, the main problem lies in the correct determination of the projected contact area of the tip. As the indents are very small, light microscopy cannot be utilized anymore for measuring them and while electron microscopy would be applicable, it is rather time consuming and expensive. Also, analysis methods have to consider the possible ocurrence of pile up which, while being of negligible effect for larger indents, can strongly affect the results obtained from NI experiments. The following section gives a short summary of the theoretical background of NI.

Nanoindentation as Advancement of Hardness Testing at Smaller Scales

At the end of the 19th century, Hertz was one of the first to treat the problem of elastic contact of two solids and, though meanwhile proven incorrect in various points, his work still builds the basis for the treatment of elastic displacement under load. Hertz was able to show that the size as well as the shape of the contact area follow from the elastic deformation of the samples. However, he neglected adhesive forces which were shown to be of significant influence to the area of contact for loads close to zero. A model worked out by Johnson, Kendall and Roberts (1971), known as the JKR model, also accounts for adhesive forces and is by now the standard model for elastic contact of solid materials. Further input came from Sneddon (1965), who worked on the relationship of load, displacement and contact area for punch geometries which could be described through the revolution of a smooth function. He proposed a powerlaw relationship between load and displacement for NI tests as

$$P = \alpha h^m \tag{8}$$

where P is the applied load, h is the elastic displacement and α and m are constants depending on the specific shape of the indenter tip.

Based on this finding and further work by Johnson (1970), Oliver and Pharr (1992; 2004) describe a method for derivation of modulus of elasticity and hardness through analysis of the unload curve from a full load/unload cycle. Figure 4 shows a representative force-displacement diagram obtained through indentation in the adhesive.

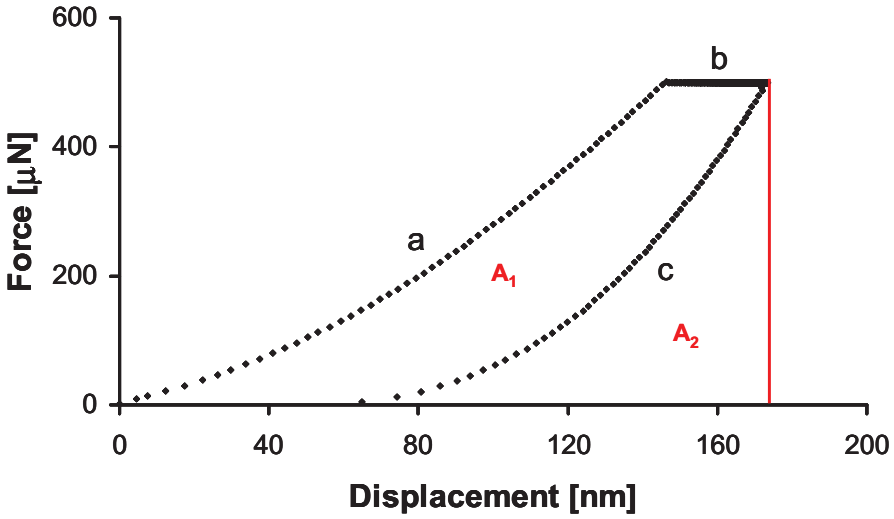

Figure 4: Representative force-displacement diagram, consisting of a) load phase, b) hold phase and c) unload phase.

During the first phase (a), the indenter tip is pressed into the tested material at a specified velocity (displacement control) or load rate (load control). At this stage, elastic, plastic and viscoelastic behaviour takes place. Reaching peak load, the tip is held for some time at a constant load to allow for visco-elastic behaviour to settle (b). This is done to provide a purely elastic unload curve (c). Its slope gives the reduced elastic modulus. The area within the curve (A_1), obtained through numerical integration, gives the work spent on plastic and visco-elastic deformation, while the area defined by the unload segment and a parallel to the force-axis gives the work of elastic deformation (A_2). While the depicted curve was obtained using load-control mode, in general the same steps are used with displacement control mode, however the shape of the curve changes slightly (see figure 19 on page 54).

To account for a non-perfectly rigid behaviour of the indenter, the reduced modulus, E_r, is defined as

$$\frac{1}{E_r} = \frac{\left(1-\nu^2\right)}{E} + \frac{\left(1-\nu_i^2\right)}{E_i} \tag{9}$$

where E and ν are the modulus of elasticity and Poisson's ratio for the specimen. ν_i and E_i are the respective values for the indenter. With the definition

of the stiffness S as derivative of the elastic unload curve ($S = \frac{dP}{dh}$), one can write E_r as

$$E_r = \frac{\sqrt{\pi}}{2} \frac{S}{\sqrt{A}} \tag{10}$$

with the contact area A. The hardness H is defined as the mean pressure supported by the material under load and therefore

$$H = \frac{P_{max}}{A} \tag{11}$$

with P_{max} the peak load.

Some annotations should be made here. First, equations (8), (10) and (11) are only valid for elastic displacement. This can be achieved by performing a number of load/unload cycles before collecting the data for analysis and inserting a few seconds hold phase before unloading to allow for visco-elastic behaviour to settle (figure 4). Also, since the unload curve is not linear, the stiffness should be calculated at the maximum load and displacement P_{max} and h_{max}. The third problem lies in the correct determination of the contact area. As explained above, microscopical methods are no real option of solving this problem.

Therefore, numerical methods to determine the contact area from the indentation data, based on an iterative approach, have been developed. The method described below is based on the assumption of the elastic modulus being independent of the indentation depth (Oliver and Pharr, 1992, 2004). Starting with several data points over a range of depths, the determination of the contact area goes as follows.

Modeling the sample and the indenter as two springs in series, the total compliance C of the system can be written as

$$C = C_s + C_i \tag{12}$$

with C_s the compliance of the sample and C_i the compliance of the indenter. The specimen compliance can be written as the inverse of the stiffness

S. Therefore, by rewriting (10) and inserting it in (12), one gets the total compliance as

$$C = C_i + \frac{\sqrt{\pi}}{2E_r}\frac{1}{\sqrt{A}} \tag{13}$$

Therefore, if the modulus is constant, a plot of C vs $A^{-\frac{1}{2}}$ gives a straight line with C_i being the intersection with the y-axis.

Rewriting (13) gives an explicit expression for the contact area

$$A = \frac{\pi}{4}\frac{1}{E_r^2}\frac{1}{(C - C_i)^2} \tag{14}$$

The true contact area is then derived interatively by fitting the experimental data according to

$$A(h_c) = \sum_{n=0}^{8} C_n h_c^{\frac{2}{2^n}} \tag{15}$$

with constants C_n and the contact depth h_c.

The starting value for the iteration process is the zero order of the above sum, a value given by the nominal tip geometry for large indents. The values for A are then inserted in (13) and from there a new function $A(h_c)$ is calculated with (14). This process gets repeated until convergence.

However, the determination of tip area function and machine compliance are largely automated processes and indenter manufacturers provide the means and guidelines for this process nowadays, so none of the above calculations had to be done manually.

Cross Sectional Nanoindentation for Characterisation of Adhesive Bond Strength

Cross sectional nanoindentaion (CSN) was introduced by Sánchez *et al.* (1999) as a new technique for adhesion characterisation of thin films at a

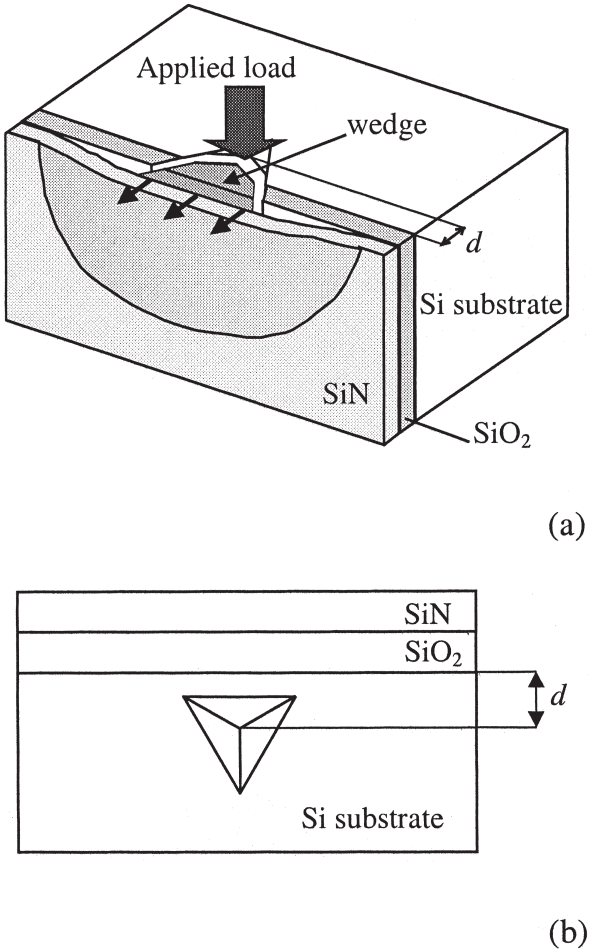

Figure 5: Schematic represantation of (a) the CSN test configuration, and (b) orientation and placement of the indentation for the experiment by Sánchez *et al.*, taken from the original paper

nanometre scale. Their work was motivated by the necessity in modern microelectronics to be able to measure adhesion at a very small scale. Therefore, their samples consisted of a tow-layer structure of Si_xN_y and SiO_2, both $1\mu m$ in diameter, brought onto a Si substrate via chemical vapour deposition. Performing indents on the sample cross section into the substrate close to the bond line, they generated a crack which grew and eventually reached and propageted along the weakest bonded interface. Figure 5 shows the original sample structure and experimental setting used.

With the debonding area (measured via scanning electron microscopy, SEM) known, the critical energy release rate was calculated. This was then compared to theoretical calculations, based on the elastic plate model, which showed very good correlation.

The technique was then further improved by Elizalde *et al.* (2003) and Molina-Aldareguia *et al.* (2007) to make it applicable to metal-ceramic interfaces and patterned structures, respectively.

Materials and Methods

This section describes the methodological aspects of the experiments undertaken within the scope of this thesis. Information on sample preparation, the various tests performed as well as analysis and interpretation of the results is provided. Sample preparation consisted basically of 3 steps, those being surface treatment with various silanes and, following that, preparation of shear test and NI samples. Tests performed were contact angle measurements, a shear test to provide a macroscopic characterisation of adhesion for comparative means and the NI experiments. Analysis consisted mostly of statistical evaluation of the gathered data.

Sample Preparation

All specimens used for silylation were spruce wood (Picea abies) with dimension $50 \times 10 \times 5$mm and $60 \times 20 \times 5$mm respectively. In order to minimize anatomical variations in samples, all samples were cut from one piece of wood. Fibre direction was parallel to the long side of the samples with vertically running annual rings (figure 6). Specimens were split into four sets, one remaining untreated and providing reference data while the other three were subjected to different surface treatments with silanes in order change surface polarity, assessed through contact angle measurement, and thus the adhesion quality. In a final step, samples were glued for shear testing and NI specimens were prepared.

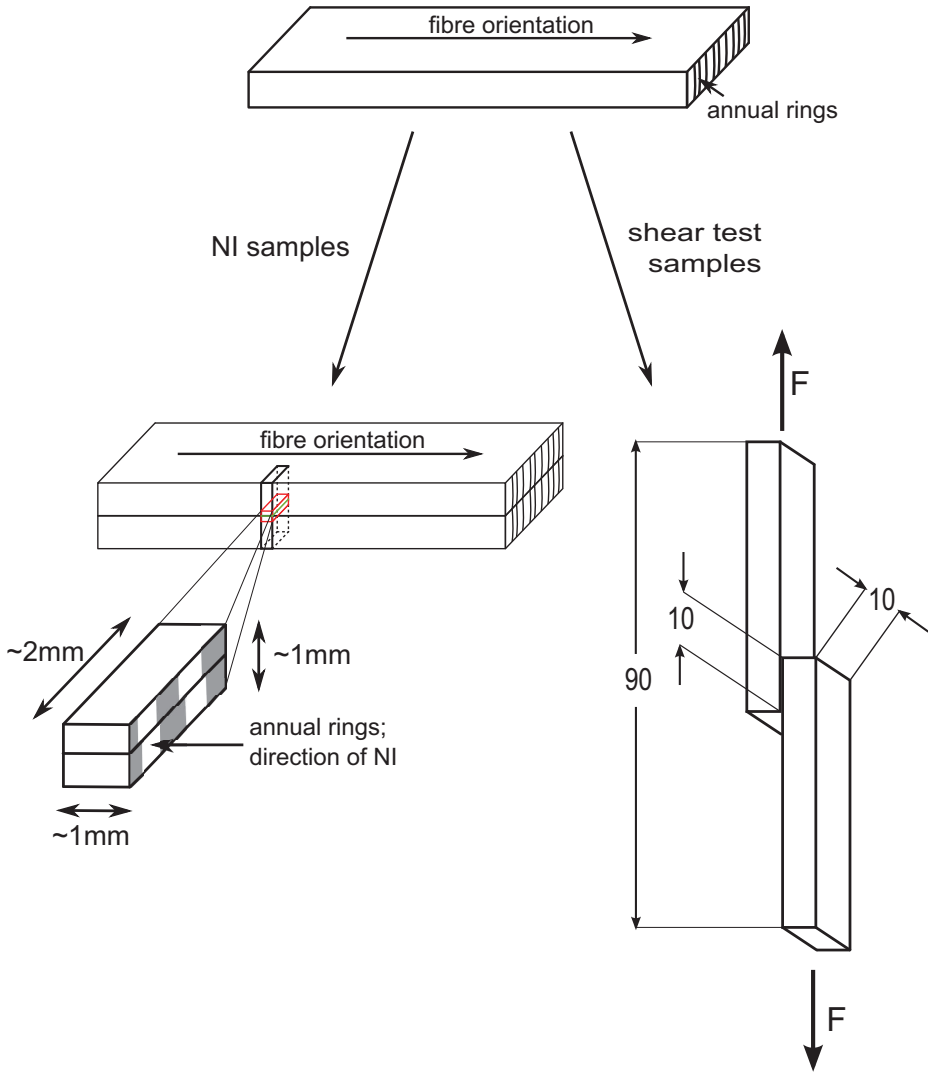

Figure 6: Schematic represantation of sample preparation and geometry.

Silylation

Silylation is the treatment of a substance with a silanes, thus substituting reactive groups of the substance with a silyl group $(-SiR_3)$ and effectively changing the surface polarity and wettability. This is often done as a means of surface protection or in order to improve adhesion. Here, the silanes were applied for the opposite reason. The silanes should substitute the cellulose's hydroxyl groups and thus lower surface polarity and give an artificially lowered adhesion with the urea-formaldehyde adhesive used for this work.

Three different silylations were performed, following methods described by Mohammed-Ziegler *et al.* (2006) and Hansmann *et al.* (2005). The agents used were γ-aminopropyltriethoxysilane (APTES) (Lactan, 97.0%), dichlorodiphenylsilane (DPS) (Sigma-Aldrich, 97.0%), octadecyltrichlorosilane (OTS) (Sigma-Aldrich, 90.0%) and chlorotrimethylsilane (CTMS) (Sigma-Aldrich, 99.0%), respectively. Solutes employed were n-hexane (Lactan, 98%) and cyclohexane (Sigma-Aldrich, 99.5%) respectively as well as small amounts of pyridine (Sigma-Aldrich, 99.9%). In advance to any further treatment, samples were kiln-dried for 24 hours at 103 ℃. For all treatments, the solution-volume to sample-surface-area ratio was 4 to 3. Below, a short discription of the different procedures is given in alphabetical order of the respective silanes.

APTES: The kiln-dried samples were swelled in cyclohexane for 20 minutes at 60 ℃. Subsequently, APTES as well as small amounts of CTMS and pyridine were added dropwise up to a concentration of 1% APTES (v/v) . The samples were left in the solution for three hours under continous stirring. After that time, samples were rinsed with cyclohexane and kiln-dried for 24 hours at 103 ℃.

DPS: Samples were left for one hour in a 1%-n-hexane-solution (v/v) under continous stirring before being rinsed with n-hexane and left to dry.

OTS+CTMS: The third procedure was a 2-step modification. To begin with, samples were treated in a 1% solution (v/v) of OTS in n-hexane. After being rinsed with n-hexane and being left to dry at ambient air for three days, the second step was a one hour treatment with CTMS (1% solution (v/v) in n-hexane). Following this, samples were rinsed with n-hexane and left to dry.

Before any further steps were taken, namely contact angle measurements and gluing of the samples, all samples were conditioned in standard climate (20℃/65% relative air humidity) for at least three days.

Preparation of Samples for Shear Testing and Nanoindentation

Following silylation treatment and contact angle measurement, samples were glued for further use. The glue used was an urea-formaldehyde-based (Prefer 10F152, Dynea) particle board glue with ammonium nitrate added as hardener. Curing was carried out in an oven for 15 minutes at 70℃ with an applied external pressure of 30N/mm².

Shear-test samples were prepared using the $50 \times 10 \times 5$mm sized specimens, with geometry loosely following EN302-1 (2004) (figure 6, lower right). To avoid shifting of the overlap region and therefor variations of the overlap area a mould was used.

For NI samples, the large specimen type was glued at full length (figure 6, lower left). This was done in order to facilitate handling and reduce predamage. The actual NI samples were then cut from the glued specimens using a jigsaw to cut small platelets and an utility knife to reduce those to cuboids of appriximately $2 \times 1 \times 1$mm, containing the glue line. Special care was taken to keep the glue joint as free of forces as possible during this step. To provide dimensional stability of the samples, the cuboids were then embedded in a 4-component epoxy resin and cured for 18 hours at 70℃. Finally, the samples were cut with a diamond knife in an ultramicrotome to provide a smooth and undamaged surface for indentation.

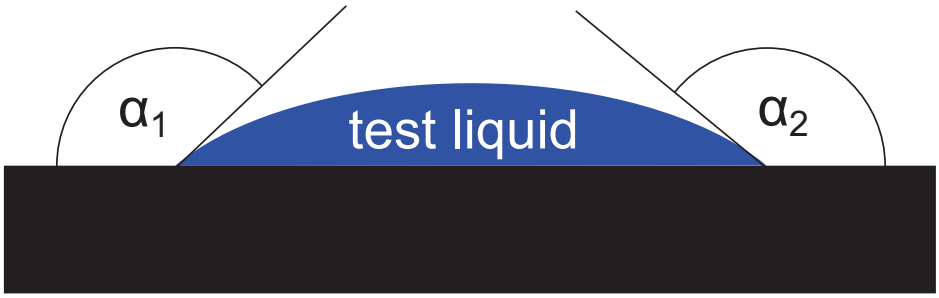

Figure 7: Schematic representation of contact angle measurement.

Experimental Methods and Analysis

Macroscopic Tests

As described in the theoretical section on page 14, the conctact angle as measure of wettability can be used to predict the adhesive quality. Therefore, using the sessile drop method described by Scheikl and Dunky (1998), the static contact angles were measured as quick and simple means of controlling the effectivenes of the performed treatments. Placing 4μl droplets of deionised water onto the flat horizontal surface with a syringe, the contact angle was determined from pictures of the doplets, taken with a camera directly attached to a light microscope. Pictures were taken right after placing the liquid on the surface (t = 0s) in intervalls of 30s at t = 0s, 30s, 60s, 90s, 120s to monitor the time dependent behaviour of the contact angle. Picture analyis was performed manually using picture analysis software (Surftens 4.3). For each sample type, 6 specimens were tested, where the value for each specimen was taken as mean of left and right contact angle (figure 7).

As the contact angle only allows for a qualitative prediction of adhesive properties, a shear test was performed to measure the actual strength. Tests were performed on a Zwick 20kN universal testing device. Samples with above described geometry were placed vertically in the decive and an increasing tension was applied until collapse. Data collection and calculation of specific shear strength, derived as peak tension over contac area, were performed automatically using firmware, only the true contact area had to be measured manually for each sample in advance to testing. For each sample type at least 10 specimens were tested.

Nanoindentation Tests

The NI tests basically consisted of three test series. For the first series, indents were performed in the adhesive and the cell wall to rule out variations in their properties taking an effect on the following experiments. The second series constituted the heart piece of this work, the actual application of CSN for adhesion measurement at the wood-adhesive interface. The third series were additionel CSN measurements with varying load functions to find out if and how the load function affects the measured results.

Material characterisation was performed with a Berkovich type indenter tip, a triangular pyramid with a total opening angle of 142.3°, with no attention given to the orientation of the tip relative to the sample. The load function utilized was a three-phase single-load function in load control mode with a 1s load phase to the peak load of 500μN, a 20s hold phase at peak load to allow for visco-elastic effects to settle and a 1s unload phase to zero load (figure 8a). For adhesive characterisation, 20-30 indents for each sample type were performed. Placement of indents was along the whole length of the bond line followed from light microscope pictures of the bond region taken in advance (figure 9a). Indents for cell wall characterisation were performed along the first row of cells without direct contact to the adhesive. Selection of cells followed from the same micrographs as above, while the actual positioning of indents on the cell wall was performed using SPM (scanning probe microscope) images of the cells taken with the indenter tip working as scanning probe. Due to the geometry of the Berkovich tip and the structure of the cell wall, the measured elastic modulus shows variations between the four walls (Konnerth *et al.*, 2009). To cancel out this effect, four indents were performed for each cell (figure 9). Properties were then calculated as mean values over all indents. For each sample type, at least 6 cells were tested, giving a minimum of 24 data points for each type.

For all CSN adhesion measurements, a cone-shaped tip with a nominal opening angle of 60° and a nominal tip radius of 150nm was used (figure 10).

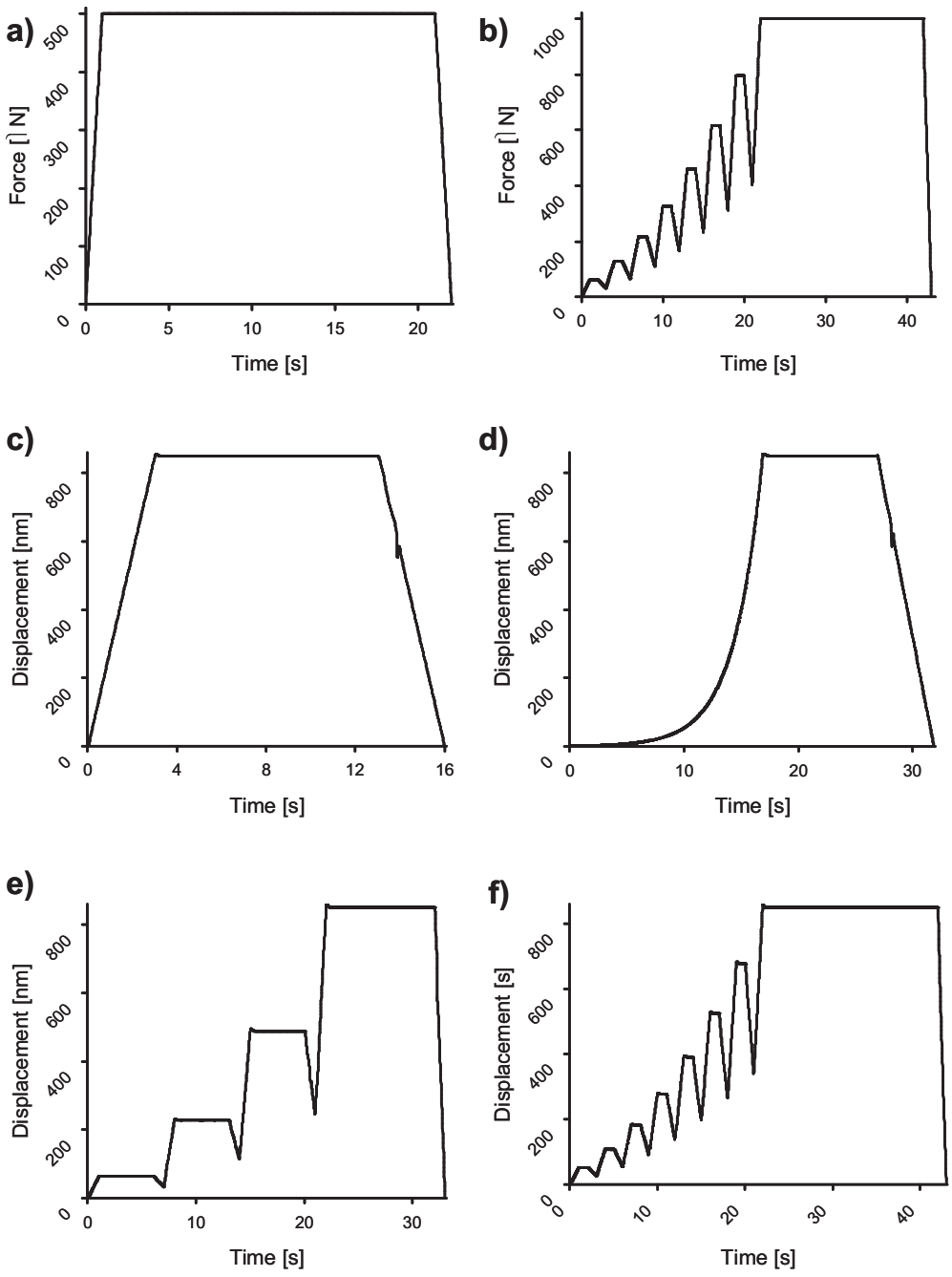

Figure 8: Load functions used for indentation work. a) load-controlled load-function for material characterisation, b) load-controlled load-function for the main CSN-experiment, c-f) displacement-controlled load-functions for analysing the influence of the load function.

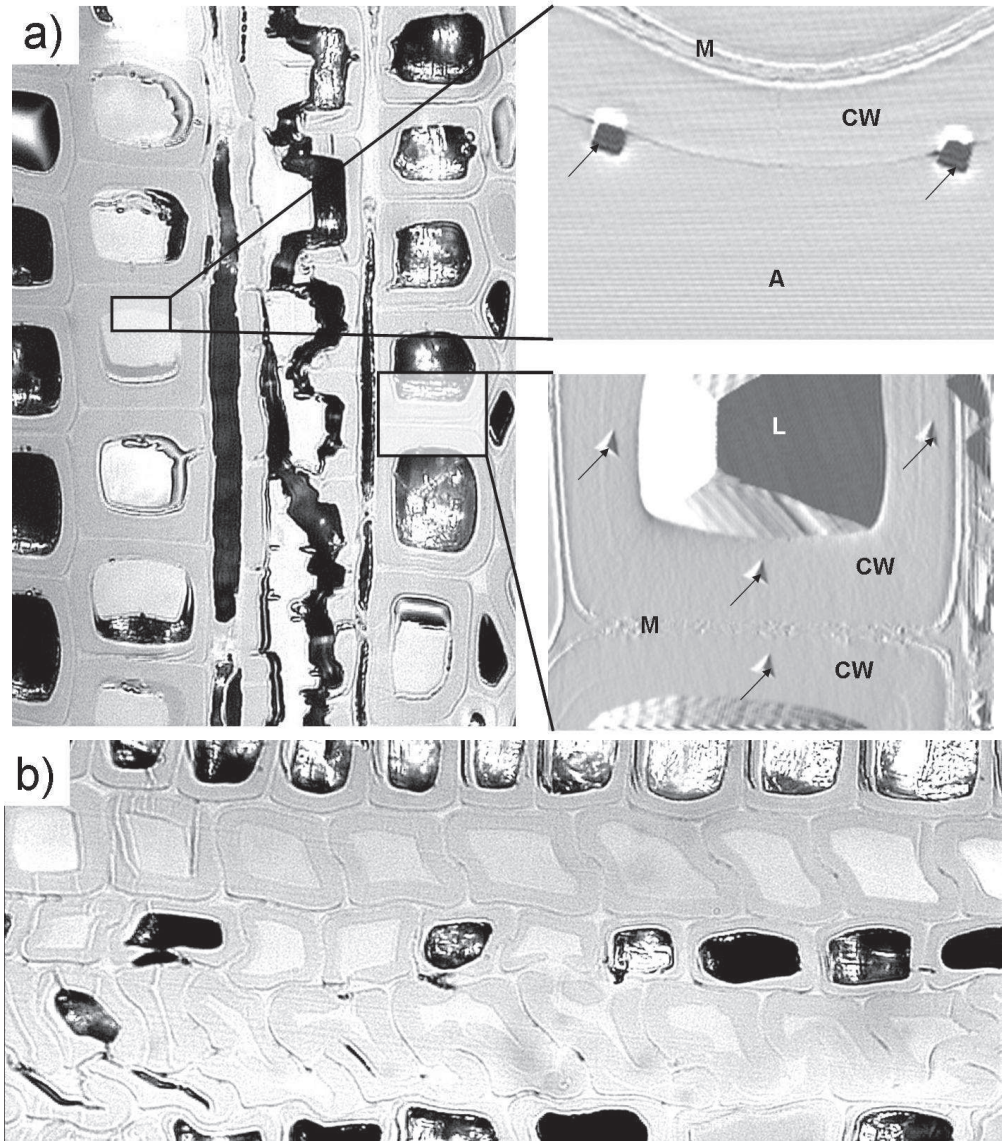

Figure 9: a) Light micrograph of a T3 sample for coarse positioning of indents (left) with representative SPM images of indents for adhesion characterisation (upper right) and cell wall characterisation (lower right), with M...middle lamella, CW...cell wall, L...lumen, A...adhesive and arrows indicating indents
b) A representative light micrograph from a reference sample for comparative means, showing the strong differences in the adhesive distribution between the sample types.

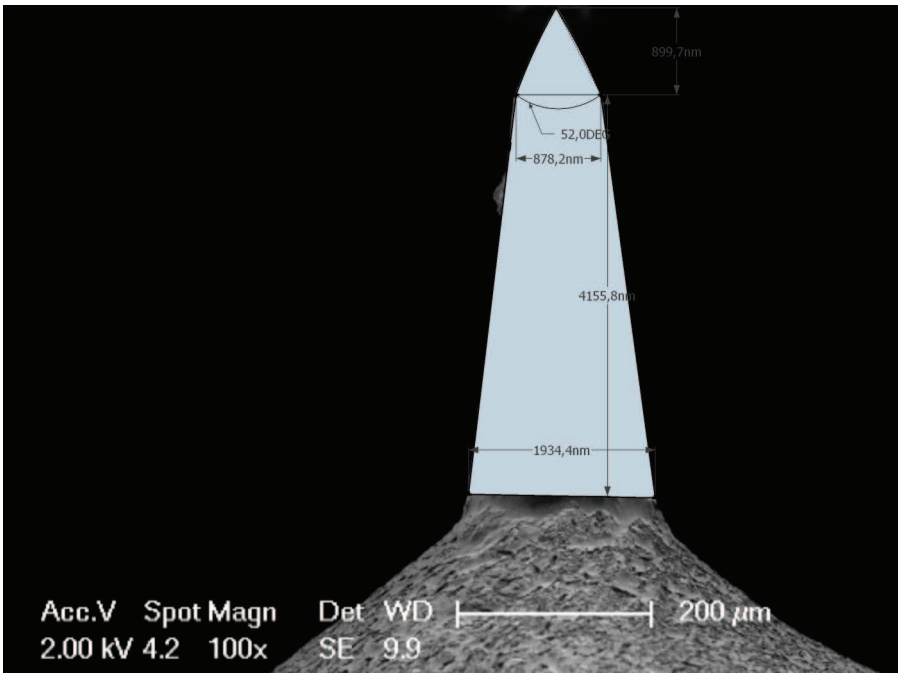

Figure 10: SEM image of cone-shaped tip for adhesion measurement

The image of the tip shows its good geometrical properties while the dirt particle visible on the left side is to high to affect the measured results. Still, the tip was cleaned and recalibrated after this image was taken.

For the second test series, the load function shown in figure 8b was used, an 8-step load function with quadratically increasing peak loads up to a final load of $1000\mu N$. The steps are added to allow for hysteresis effects to settle and relaxation of visco-elastic stresses. The final load was held for 20s before unloading to zero load.

Due to the nature of the samples used in the original test devised by Sánchez *et al.*, especially the Si substrate, crack building was guaranteed and models correlating the adhesion strength to the crack length and crack interface could be built quite well. However, introducing the technique to wood-adhesive bond lines posed several problems. First of all, due to the soft and elastic nature of both wood and adhesive, no crack propagation in the materials was to be expected. Also, the complex structure of the wood cell wall greatly complicates any mathematical modelling. Furthermore, it was to be expected that the main work of indentation would be due to plastic

and visco-elastic deformation. For these reasons, the applicability of CSN could not be taken for granted and experimental settings had to be modified by shifting the indent position from the substrate (wood) directly to the bond line. The indents were performed on cut open cells with full contact between adhesive and cell wall or, more often, in adhesive filled cells with full contact between adhesive and cell wall. For the latter, care was taken for the tested cells to have a minimum diameter of about $10\mu N$ to eliminate influences from the opposing or adjacent walls. Same as above, light microscope images were used to select fit cells while positioning of the indents followed from scanning probe microscopy (SPM) images of the region (figure 9).

The third test series, comparing different load functions, was performed on the two sets of samples which showed the strongest differences in results in the previous test. To make sure that the indentation depth would not exceed the 900nm tip length of the nominal cone (figure 10), all load functions were displacement controlled with a maximum displacement of 850nm. The load functions, depicted in figure 8c-f, were as follows:

LF1 a linear single-load function with 3s/10s/3s load/hold/unload-phase

LF2 a single-load function with a continuous quadratic displacement increase over 17s to peak displacement, followed by a 10s hold and 5s unload phase

LF3 a four step function with 1s/5s/1s load/hold/unload phases with a 10s hold phase at the fourth step, unloading to half peak displacement between steps, peak displacement increasing quadratically

LF4 an displacement controlled eight step function, the analogue to the force controlled function used in the previous test series

Apart from the load functions, experimental settings, especially positioning of indents, were the same as above. Also, the samples used were the same as for the first two test series. To prevent influences from previous setting, sample surfaces were re-cut between series 2 and 3.

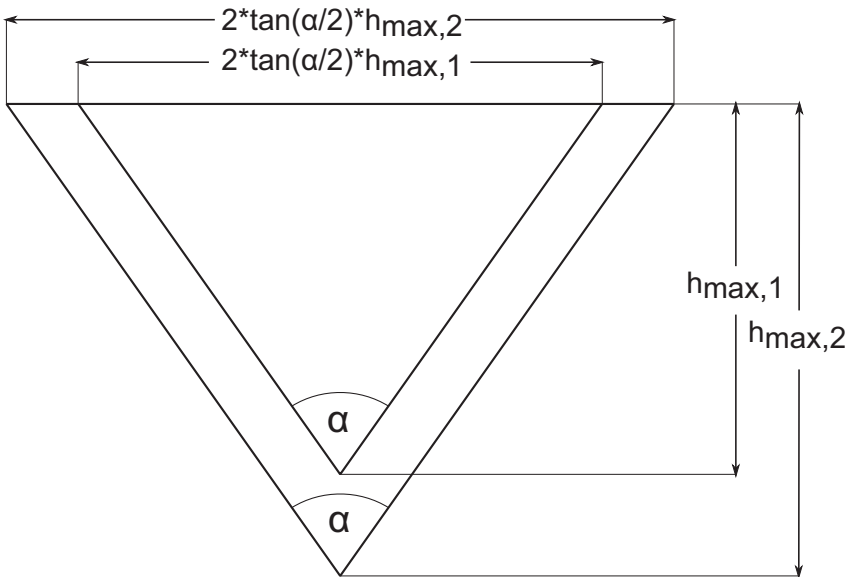

Figure 11: By assuming the debonding areas to be geometrically similar equal-sided triangles with opening angle α, the width of indents becomes a function of indentation depth as depicted. For known width to depth ratio, the area can therefore be calculated as a function of h_{max}^2, as explained in the text.

Data Analysis

Additionally to the automatically calculated values for hardness and modulus of elasticity, the specific work of debonding was determined as a measure of adhesion strength. Since no exact values for the debonded areas were available, an approximation was made by assuming the debonding areas to have the shape of geometrically similar triangles. This assumption was supported by the strong linear correlation between the maximum indentation depth, measured automatically by the testing equipment, and the width of indents, evaluated manually from SPM images of the indents.

Since the debonding areas were not measured, they were assumed to be geometrically similar triangles, which allowed the areas to be expressed as only dependent on one variable, that being indentation depth (figure 11). This assumption was supported by a strong linear correlation (figure 12) between maximum indentation depth, collected automatically by the testing device, and width of indents, evaluated manually from SPM images of the indents.

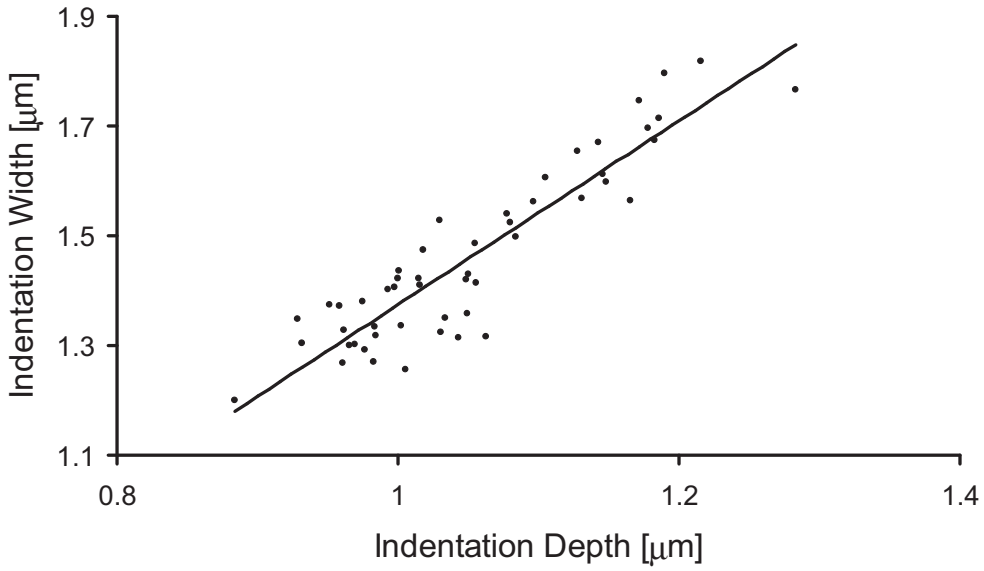

Figure 12: Linear correlation between maximum indentation depth and width of indents; $R^2 = 0.834$, 2-tailed Pearson correlation significant at 0.01 level

The specific work of debonding, $\hat{W}_D$, defined as the total work of debonding over the debonded area, can thus be expressed as

$$\hat{W}_D = \frac{W_D}{\frac{1}{2}(w_{ind} * h_{max})} = \frac{W_D}{\frac{1}{2}(c * h_{max}^2)} \tag{16}$$

where W_D is the total work of debonding,w_{ind} the width of the indents and h_{max} is the maximum indentation depth. The dimensionless constant c gives the relation between w_{ind} and h_{max}. It depends on the opening angle α of the indents as illustrated in figure 11 and is derived as the slope of the fit in figure 12.

For relative values, where the value of the reference is defined as 100%, the constants get eliminated from the equation and the results only depend on the directly measured maximum depth and the total work of debonding.

Since the load functions for the third test series were displacement controlled with $h_{max} = 850nm$, the constant c was derived as the arithmetic mean of indent widths over w_{max}. Due to a rather poor resolution of the SPM images, measuring the width of indents was quite subjective when the actual

edge of the indent was not clearly defined. To keep consistency, when in doubt, the smaller value was taken. Still, this gives an error margin of about 10-15%.

Results and Discussion

Macroscopic Tests

From here on, the labels Ref, T1, T2, T3 will be used for reference and silylated samples according to their contact angles (figure 13), therefore

Reference = Ref

APTES = T1

DPS = T2

OTS+CTMS = T3

All graphs are plotted in this order with error bars representing one standard deviation, in order to allow an easier comparison of results.

Contact angle measurements show a strong trend of increased contact angles, and therefore decreased wettability, for the various treatments. This becomes even stronger over time as samples with lower initial contact angles show a stronger time dependency (figure 13a-d).

In analogy to the trend found in figure 13, figure 14 shows a strong decrease in shear strength for increasing contact angles, where differences between the silylated samples and the reference sampe are statistically significant (T1, $p < 0.05$) and highly significant (T2, T3, $p < 0.01$) respectively. It should

be noted that the measured shear strength of 7.5MPa for the reference sample only indicates the lower limit for adhesive strength, as the failure was cohesive failure in the wood for all samples with peak loads reaching values of 11.5MPa. Therefore, numerical differences in strength between reference and modified samples are all underestimated. On the other hand, adhesive strength for T3 specimens was very low, up to a point where measuring was nearly impossible as adhesive failure occured when putting on pre-load. This allows the assumption that no adhesive bonds were built and the measured residual strength is due to purely physical forces as friction and weak molecular interactions.

Therefore, the prerequesites for the NI experiment, one set of samples with very good adhesion (reference) and one with no or hardly any specific adhesion (T3), were provided, with T1 and T2 samples for intermediate steps.

NI Tests

The results of the adhesive and cell wall characterisation are depicted in figure 15, with their exact values given in table 1. The reduced modulus of adhesive and cell wall shows only small and nonsignificant variations, while the values taken at the cell wall are in the expected range (Gindl *et al.*, 2004). The same is true for the hardness of the cell wall region. While deviations do exist, they do not follow a specific trend and are all non-significant. Only the hardness of the adhesive for T3 samples show a significant increase (33%) compared to the other sample types. In general, however, the obtained results allow the conclusion that the silylation treatments did not greatly influence the mechanical properties of the wood cell wall or those of the adhesive. Therefore, it seems justified to ascribe differences in the results from indentation tests directly at the interface to a change in specific adhesion due to a changed wettability.

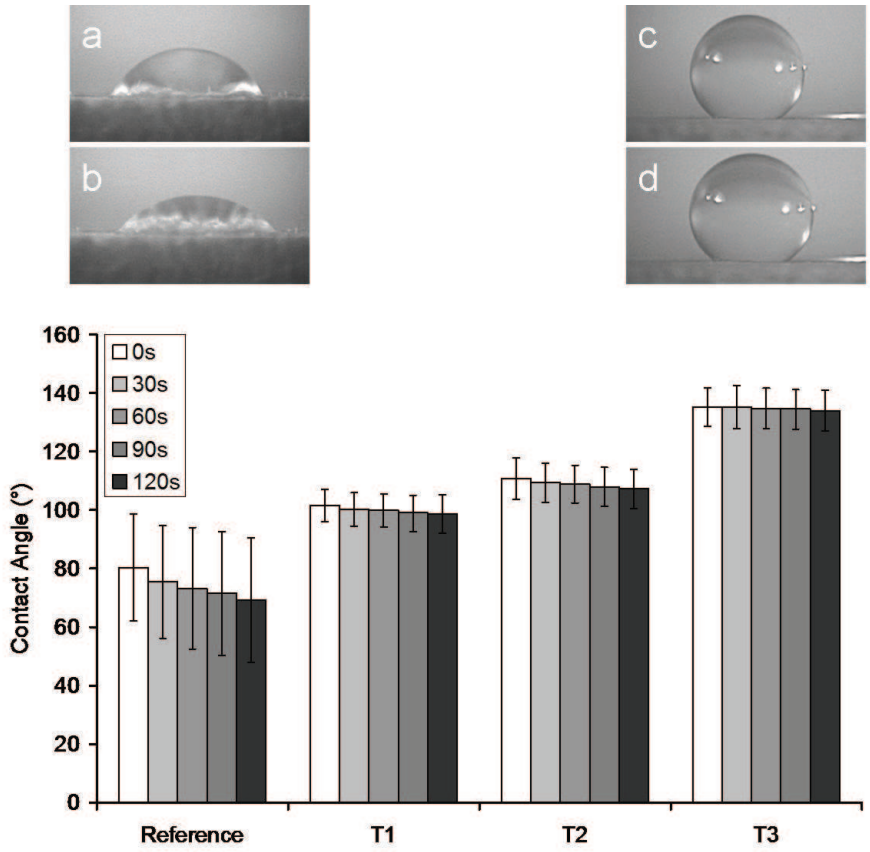

Figure 13: Results from contact angle measurement; a significant increase in contact angle is apparent for all treatments which is strongest for the T3 sample type with an increase at t = 0s of over 50°. To better illustrate the time dependency, images a-d show a liquid drop on the reference and T3 sample at t = 0s and t = 120s. While hardly any change is visible for the T3 specimen, a strong decrease is apparent on the reference sample.

	Ref	T1	T2	T3
$E_{r,Adhesive}$	20.3±2.3	20.4±1.6	20.3±0.8	19.8±1.8
$H_{Adhesive}$	0.47±0.09	0.407±0.08	0.45±0.03	0.41±0.06
$E_{r,Cell\,Wall}$	11.5±0.9	11.8±0.7	10.9±0.9	11.5±0.9
$H_{Cell\,Wall}$	0.74±0.03	0.75±0.07	0.74±0.05	0.95±0.10**

Table 1: Reduced modulus and hardness from material characterisation in the adhesive and the cell wall. All values are given in [GPa]. ** highly significant variation ($p < 0.01$) to reference value

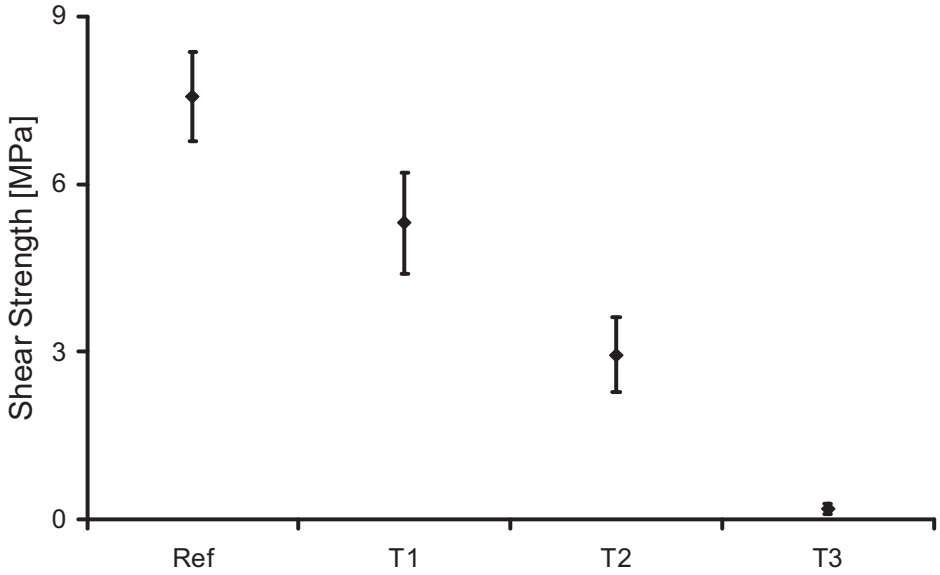

Figure 14: The shear strengh shows a strong decrease in correlation with an increasing contact angle. Special attention should be paid to the near-zero strengh of T3 samples. Due to cohesive failure in the wood, the reference value can only be seen as lower limit of the actual shear strength.

Figure 16 gives the results of indentations performed directly at the bond line. As should be expected, the elastic modulus (figure *16*a), influenced by the elastic properties of the adhering materials instead of the adhesion, mainly mirrors the properties of the adhesive and does not show significant deviations between sample types. The hardness (figure *16*b), on the other hand, shows a weak but clear trend of decreasing hardness for increasing contact angles (figure 13). Even though variations are rather small, they are significant (T2, $p < 0.05$) and highly significant (T3, $p < 0.01$). Due to the results of material characterisation, it seems justified to assume these variations as being caused by different qualities of the adhesive bond. Also, with these results the increased hardness of the adhesive in T3 samples becomes less problematic as it should, if anything, lead to an underestimation of the deviations from the other samples.

The same trend as for the hardness is apparent for the specific work of debonding (figure (17)), derived as described above (16 on page 42). With the results found in the shear test, the indentation work in the T3 sample can wholly be ascribed to deformation losses. For the reference samples, it contains an additional fraction ascribed to the specific adhesion caused by strong interactions at the interface. Therefore, the difference between the

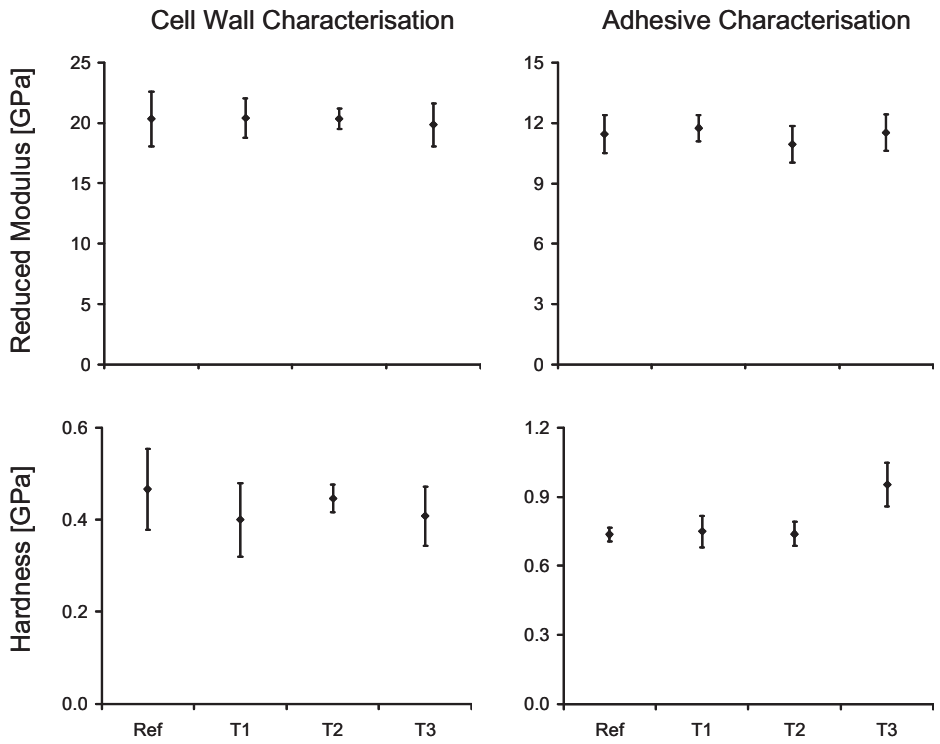

Figure 15: Results of NI tests in the cell wall and the adhesive for characterisation of their respective mechanical properties. With the exception of the increase in hardness of the adhesive for T3 samples, all variations are non-significant and no clear trends can be perceived.

mean indentation work on the reference sample (570J/m²) and the T3 sample (490J/m²) gives a measure of the specific work of adhesion (see 19b,c). These 80J/m² are considerably smaller than the 200J/m² measured with a comparable macroscopic mode 1 fracture test (Veigel *et al.*, 2010). However, this can be explained by a much smoother fracture surface for the CSN method.

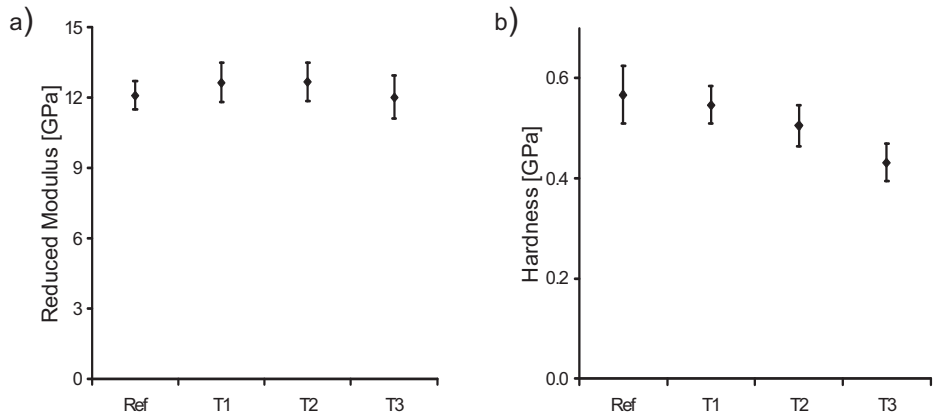

Figure 16: Modulus and hardness from indentations at the wood-adhesive interface. The reduced modulus of elasticity shows no significant variations or apparent trend (a). However, in accordance with the results from the shear test, a trend towards a decreased hardness for larger contact angles is visible (b).

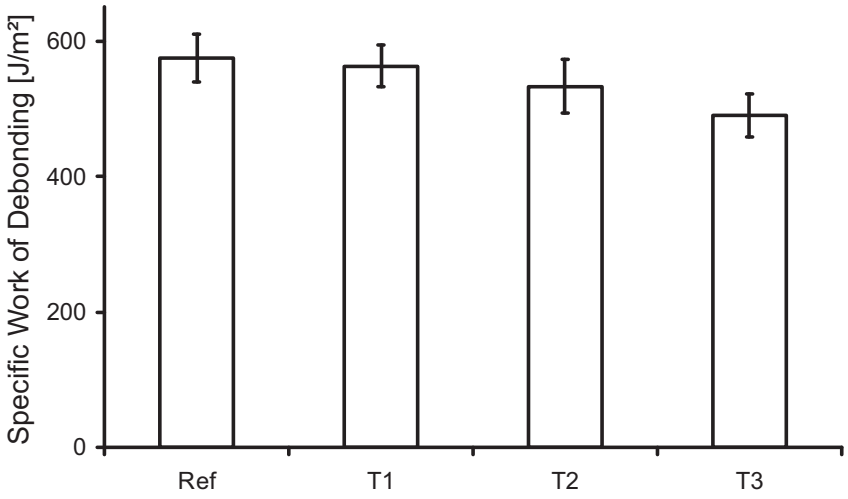

Figure 17: The specific work of debonding from indentation at the bond line. Even though it is rather weak, the same trend as for the hardness is apparent. For T2 and T3, variations to the reference are statistically significant.

	CSN_1	LF1	LF2	LF3	LF4
Ref	570±40	760±50	750±40	840±60**	990±60**
T1	560±30	-	-	-	-
T2	530±40^{+}	-	-	-	-
T3	490±30^{++}	700±90^{+}	640±80^{++}	720±120^{++}	820±240
$T3_r$	85±6^{++}	92±12^{+}	85±11^{++}	85±15^{++}	83±24

Table 2: Specific work of debonding in [J/mm²] for all indentation tests performed directly at the bond line (CSN_1...first, load controlled experiment; LF1-4...experiments with varying load functions). $T3_r$...relative values in T3 sample; **...highly significant variation ($p < 0.01$) to values in the same row; $^{+}$...significant variation ($p < 0.05$) to the reference value; $^{++}$...highly significant variation ($p < 0.01$) to the reference value

One might take notice that the mean peak indentation depth (1000-1200nm) for all samples is in excess of the actual tip zone with a length of 900nm. However, due to the geometry of the tip (figure 10), this should have no or hardly any effect on the results insofar, as all indents are influenced the same way. Comparison of the relative values for the specific work of debonding (table 2) with the results derived with different, displacement controlled load functions, support this assumption. Still, the loss of contact is the most likely cause for a significantly lowered specific work of indentation when compared to the latter displacement controlled indentations, as it greatly reduces the work spent on plastic and visco-elastic deformation.

For the third test series, only the work of indentation was calculated. All load functions show the expected decreased work of indentation for the T3 sample type. This decrease to about 85% of the reference sample value for L2-L4 is about the same as for the above test. For LF1, this variation is with an 8.5% margin clearly, if non-significantly, weaker (figure (18)a). Significant differences between the results are obvious when considering the absolute values (figure (18)b).Here, an increased specific work is apparent for multible load phases, being highly significant ($p < 0.01$) for LF2-LF3 and LF3-LF4 (alternately for LF1-LF3, too). For the treated samples, only the step LF2-LF3 is significant ($p < 0.05$) due to the large standard deviation for LF4. This increased standard deviation is most likely caused by a low number of indents ($n = 10$) combined with an unlucky choice of indent positions.

The results indicate that the used load function does indeed have an influ-

ence on the outcome of the tests. The reduced margin between the two samples found for LF1 should be due to the rather short load phase and resulting high load velocity, since it reduces the propability of the debonding to properly occur at the interface (as its weakes point) but rather only close to the interface in the material. To some point, this can also explain the increased work of indentation for multible load steps. However, the more significant part of this increase is due to an increased energy loss on plastic and visco-elastic deformation, caused by hysteresis effects during the unload-reload phase (figure 19).

This increase causes a problem for the comparability of results. As the relative values all showed about the same magnitude of variation, absolute variation increases with the total work spent. This led to the specific work of adhesion varying by more than a factor of 2 (80J/m^2 to 170J/m^2). Therefore, results should only be compared for identical load functions, while comparison with macroscopic results is limited to the order of magnitude.

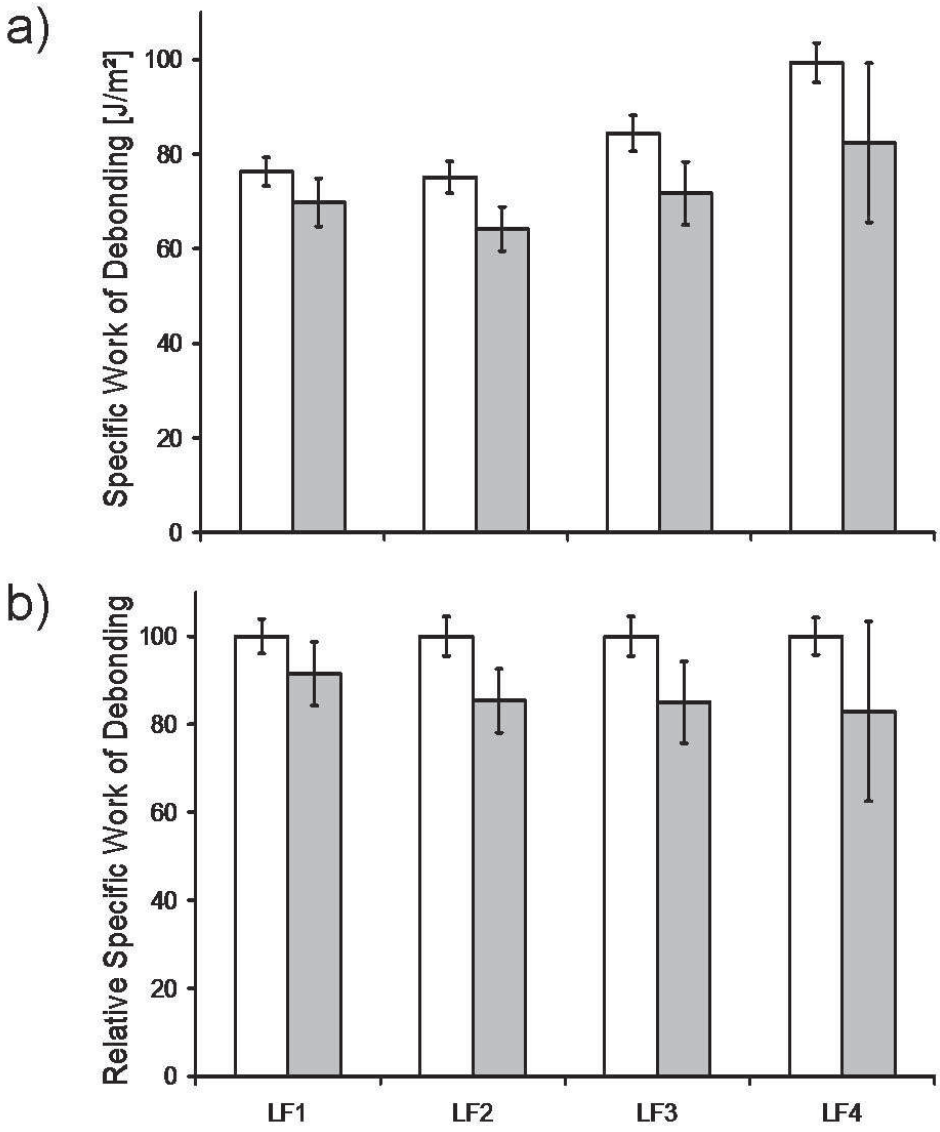

Figure 18: Comparison of the specific work of debonding for reference (white blocks) and T3 (grey blocks) samples for different load functions. An increase in the work of debonding using multible load/unload cycles is visible (a). Still, with the exception of LF1, the variation of the relative values is about the same.

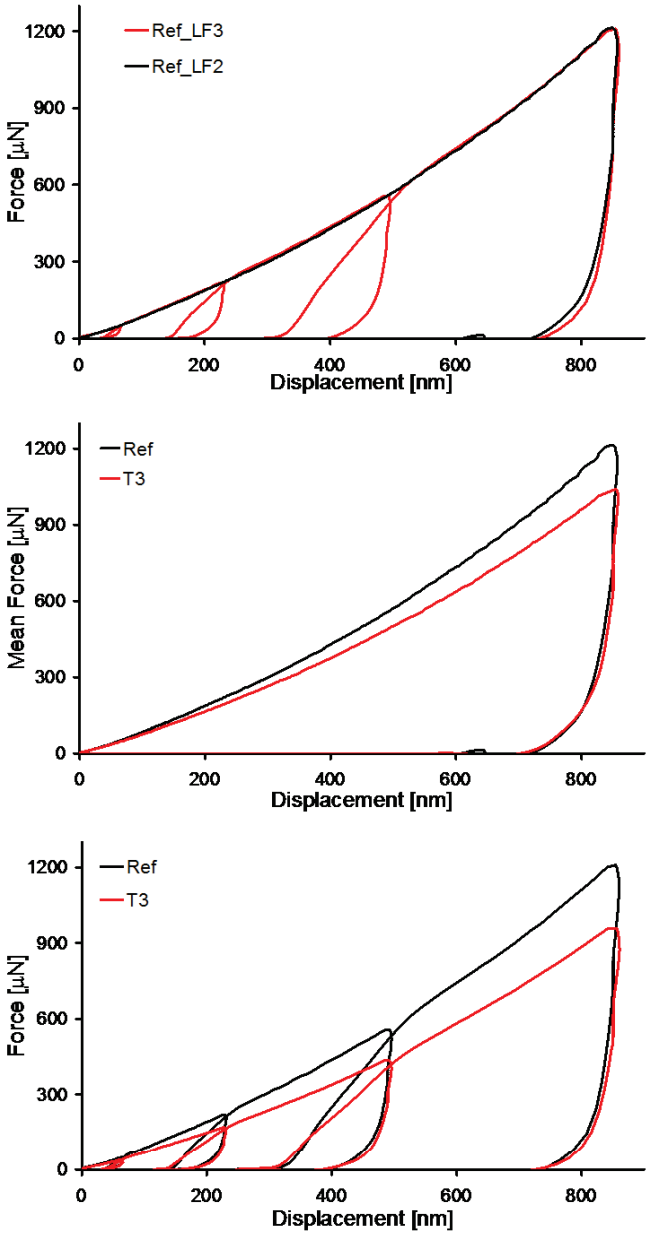

Figure 19: a) Comparison between the mean load-displacement graphs for LF2 and LF3 on the reference sample. A strong hysteretic behaviour for LF3 is apparent, causing an increased work of indentation. b, c) Comparison of the mean load-displacement graphs on the reference and T3 sample for LF2 and LF3 respectively. The area between the curves gives ameasure of the specific adhesion.

Conclusion

In the scope of this work, CSN was successfully applied to measure the adhesion at the interface between wood and an urea-formaldehyde adhesive. Comparing the results between a sample with an artificially lowered adhesion close to zero and an untreated reference sample, it was possible to deduce the specific work of adhesion at the interface. However, further experiments indicated that this is strongly dependent on the applied load function, varying by more than a factor of 2. To prevent this problem, it might be usefull for future experiments to find out about a convergence limit of the indentation work (and the specific work of adhesion) for a higher number of steps. The second problem that still remains is the proper determination of the delaminated area. Due to its dependence on the residual width, the specific work of adhesion is incluenced by another highly uncertain value, again limiting the comparability of results to other test methods.

Without further knowledge about how delamination takes place in the sample, the use of CSN data is limited to comparison only with itself, as comparison to data from other tests are meaningless as long as we do not know how the specific adhesion changes with the test procedure.

Still, CSN should prove a valuable asset in researching adhesion at wood-adhesive interfaces. The possibility to monitor changes of specific adhesion for varied parameters on a cell wall level should, in combination with macroscopic test methods, provide new insights in failure processes in wood-adhesive systems and further our understanding thereof.

Therefore, further work should aim for the application of CSN to a wide variety of adhesive systems and a better understanding of the deformation processes ocurring for CSN.

Appendix

Curriculum Vitae

Ausbildung

- 09/1992 – 06/2004
  Schulausbildung an der Volksschule Friesach und dem BG/BRG St. Veit/Glan
- 06/2004
  Matura am BG/BRG St. Veit/Glan
- 10/2005 – 05/2011
  Diplomstudium Physik an der Universität Wien, mit Auslandsaufenthalt in Swansea/Wales von 02/2009 – 05/2009
- 10/2007 – 01/2009 und 10/2009 – 04/2011
  Mitbelegung von Kursen an der Universität für Bodenkultur Wien im Rahmen des Bachelorstudiums Holz- und Naturfasertechnologie

Praktische Erfahrungen

- 12/2005 – 08/2008
  Nachhilfelehrer (Schwerpunkt Mathematik) am WILK Lernhilfeinstitut
- 2006 – 2011
  Diverse Praktika (Laborübungen) am Institut für Physik im Rahmen des Studiums, dabei Arbeiten an STM, STEM, SEM und Raman Spektrometer sowie Feinstrukturanalyse mittels Röntgenstreuung

- 02/2010
  Praktikum am Institut für Holzforschung der Universität für Bodenkultur Wien
- 06/2010 – 04/2011
  Diplomarbeit am Institut für Holzforschung der Universtität für Bodenkultur Wien im Rahmen des Diplomstudiums Physik

List of Figures

Bibliography

A. N. Gent, and J. Schultz, 1971.

Bikerman, J., 1968, *Science of Adhesive Joints* (Academic Press), ISBN 0120978520.

Brown, H., 1989, Macromolecules **22**(6), 2859.

Brown, H., 1991, Macromolecules **24**(10), 2752.

Brown, H., V. Deline, and P. Green, 1989, Nature **341**(6239), 221.

C1624-05, A., 2010, *Standard Test Method for Adhesion Strength and Mechanical Failure Modes of Ceramic Coatings by Quantitative Single Point Scratch Testing*.

C794-10, A. C., 2010, *Standard Test Method for Adhesion-in-Peel of Elastomeric Joint Sealants*.

D1002-10, A., 2010, *Standard Test Method for Apparent Shear Strength of Single-Lap-Joint Adhesively Bonded Metal Specimens by Tension Loading (Metal-to-Metal)*.

D3163-01, A., 2008, *Standard Test Method for Determining Strength of Adhesively Bonded Rigid Plastic Lap-Shear Joints in Shear by Tension Loading*.

D3330-04, A., 2010, *Standard Test Method for Peel Adhesion of Pressure-Sensitive Tape*.

D3762-03, A., 2010, *Standard Test Method for Adhesive-Bonded Surface Durability of Aluminum (Wedge Test)*.

D5868, A., 2008, *Standard Test Method for Lap Shear Adhesion for Fiber Reinforced Plastic (FRP) Bonding*.

Delescluse, P., J. Schultz, and M. Shanahan, 1984, in *Adhesion (Barking, England)*, pp. 79–96.

Deryagin, B., and N. Krotova, 1948, DOKLADY AKADEMII NAUK SSSR **61**(5), 849, ISSN 0002-3264.

DiFrancia, C., T. C. Ward, and R. O. Claus, 1996, Composites Part a-Applied Science and Manufacturing **27**(8), 597, ISI Document Delivery No.: UX421 Times Cited: 30 Cited Reference Count: 75.

DIN53254, 1987, *Prüfung von Holzklebstoffen Bestimmung der Klebfestigkeit von Längsklebungen im Scherversuch*.

Dupré, A., and P. Dupré, 1869, *Théorie mécanique de la chaleur* (Gauthier-Villars).

Elizalde, M. R., J. M. Sánchez, J. M. Martínez-Esnaola, D. Pantuso, T. Scherban, B. Sun, and G. Xu, 2003, Acta Materialia **51**(14), 4295–4305.

EN1071-05, D., 2005, *Advanced technical ceramics - Methods of test for ceramic coatings - Part 3: Determination of adhesion and other mechanical failure modes by a scratch test*.

EN205, E. N., 1997, *Klebstoffe - Holzklebstoffe für nichttragende Anwendungen - Bestimmung der Klebfestigkeit von Längsklebungen im Zugversuch* (ersetzt durch ÖNORM EN205 von 1997 Ersatz für ÖNORM EN205 von 1992), ISBN ICS 83.180, ersatz für ÖNORM EN205: 1992-06.

EN302-1, N., 1992, *Klebstoffe für tragende Holzbauteile Prüfverfahren Bestimmung der Klebefestigkeit durch Längszugscherprüfung* (ersetzt durch Önorm EN302-1 von Oktober 2004).

EN302-1, N., 2004, *Klebstoffe für tragende Holzbauteile - Prüfverfahren, Teil 1: Bestimmung der Längszugscherfestigkeit* (Ersatz für ÖNORM EN302-1 von 1992), ICS 83.180.

EN302-4, N., 1992, *Klebstoffe für tragende Holzbauteile Prüfverfahren Bestimmung des Einflusses von Holzschwindung auf die Scherfestigkeit* (ersetzt durch ÖNORM EN302-4 von Oktober 2004).

Fowkes, F., and S. Maruchi, 1977, Abstracts of papers of the american chemical society **173**(MAR20), 110, ISSN 0065-7727.

Fowkes, F., and M. Mostafa, 1978, Industrial and Engineering Chemistry Product Research and Development **17**(1), 3.

Fowkes, F. M., 1984, Rubber Chemistry and Technology **57**(2), 328.

Fowkes, F. M., 1987, Journal of Adhesion Science and Technology **1**(1), 7.

Gindl, W., H. Gupta, T. Schöberl, H. Lichtenegger, and P. Fratzl, 2004, Applied Physics A: Materials Science and Processing **79**(8), 2069–2073.

Hansmann, C., G. Weichslberger, and W. Gindl, 2005, Wood Science and Technology **39**(6), 502–511, ISSN 0043-7719.

Hertz, H., 1895, *Schriften Vermischten Inhalts*.

Johnson, K., 1970, Journal of the Mechanics and Physics of Solids **18**(2), 115, ISSN 0022-5096.

Johnson, K. L., K. Kendall, and A. D. Roberts, 1971, Proceedings of the Royal Society of London. Series A, Mathematical and Physical Sciences **324**(1558), 301, ISSN 00804630, ArticleType: research-article / Full publication date: Sep. 8, 1971 / Copyright © 1971 The Royal Society.

Jud, K., H. Kausch, and J. Williams, 1981, Journal of Materials Science **16**(1), 204.

Kim, Y., and R. Wool, 1983, Macromolecules **16**(7), 1115.

Konnerth, J., N. Gierlinger, J. Keckes, and W. Gindl, 2009, Journal of Materials Science **44**(16), 4399–4406.

McBain, J., and D. Hopkins, 1925, JOURNAL OF PHYSICAL CHEMISTRY **29**(2), 188, ISSN 0022-3654.

Miller, B., P. Muri, and L. Rebenfeld, 1987, Composites Science and Technology **28**(1), 17, ISSN 0266-3538.

Mohammed-Ziegler, I., Z. Hórvölgyi, A. Tóth, W. Forsling, and A. Holmgren, 2006, Polymers for Advanced Technologies **17**(11-12), 932–939.

Molina-Aldareguia, J. M., I. Ocaña, D. González, M. R. Elizalde, J. M. Sánchez, J. M. Martínez-Esnaola, J. Gil-Sevillano, T. Scherban, D. Pantuso, B. Sun, G. Xu, B. Miner, *et al.*, 2007, Engineering Failure Analysis **14**(2), 349–354.

Nardin, M., E. Asloun, and J. Schultz, 1991, Surface and Interface Analysis **17**(7), 485.

Nardin, M., A. E. Maliki, and J. Schultz, 1993, The Journal of Adhesion **40**(2), 93, ISSN 0021-8464.

Oliver, W. C., and G. M. Pharr, 1992, Journal of Materials Research **7**(6), 1564–1580.

Oliver, W. C., and G. M. Pharr, 2004, Journal of Materials Research **19**(1), 3–20.

Packham, D. E., 2003, in *Handbook of Adhesive Technology*, edited by A. Pizzi and K. L. Mittal (Marcel Dekker, Inc., Krems, Austria), 2 edition, p. 69–93.

Prager, S., and M. Tirrell, 1981, The Journal of Chemical Physics **75**(10), 5194.

Sargent, J., 2005, International Journal of Adhesion and Adhesives **25**(3), 247, ISSN 0143-7496.

Scheikl, M., and M. Dunky, 1998, Holzforschung **52**(1), 89–94.

Schultz, J., and A. Carré, 1984, Applied Polymer Symposia (39), 103, ISSN 0570-4898.

Schultz, J., A. Carré, and C. Mazeau, 1984, International Journal of Adhesion and Adhesives **4**(4), 163.

Schultz, J., L. Lavielle, A. Carre, and P. Comien, 1989, Journal of Materials Science **24**(12), 4363.

Schultz, J., K. Tsutsumi, and J. Donnet, 1977, Journal of Colloid And Interface Science **59**(2), 277.

Sánchez, J., S. El-Mansy, B. Sun, T. Scherban, N. Fang, D. Pantuso, W. Ford, M. Elizalde, J. Martínez-Esnaola, A. Martín-Meizoso, J. Gil-Sevillano, M. Fuentes, *et al.*, 1999, Acta Materialia **47**(17), 4405–4413.

Sneddon, I., 1965, International Journal of Engineering Science **3**(1), 47.

Vasenin, R., and V. Saltykova, 1975, Soviet Materials Science **9**(5), 552.

Veigel, S., J. Follrich, W. Gindl-Altmutter, and U. Müller, 2010, Comparison of fracture energy testing by means of double cantilever beam-(DCB)-specimens and lap joint testing method for the characterization of adhesively bonded wood.

Wake, W. C., 1982, *Adhesion and the formulation of adhesives, second edition*.

Young, T., 1805, Philosophical Transactions of the Royal Society of London **95**, 65 .

Zhandarov, S., and E. Mäder, 2005, Composites Science and Technology **65**(1), 149, ISSN 0266-3538.